doi.org/10.36721/PJPS.2023.36.5.SP.1573-1582.1

Development and characterization of polyamidoamine based doxorubicin loaded polymeric nanocarriers and *in-vitro* evaluation on liver cancer cell lines

Nadia Mazhar, Zeeshan Danish* and Hamid Saeed
Punjab University College of Pharmacy, University of the Punjab, Lahore, Pakistan

Abstract: In order to achieve the benefits of targeted drug delivery, this study intended to encapsulate doxorubicin in a linear polyamidoamine and its PEGylated co-polymer. The drug was loaded by using the emulsion solvent evaporation method. By adjusting the doxorubicin to polymer ratios to 1:10, 1:20 and 1:30, three formulations of each polymer/copolymer were prepared. The drug release profile was investigated using phosphate buffered saline. *In vitro* cytotoxicity investigation was executed on liver cancer cell line (Hep G2 cell lines) by 3-[4,5-dimethylthiazol-2-yl]-2,5 diphenyl tetrazolium bromide assay. The outcome demonstrated that doxorubicin had been successfully loaded on polyamidoamine and its PEGylated co-polymer with a drug loading efficiency of about 90%. Nanocarrier sizes were between 245±1.10 nm -579±1.00 nm and the zeta potential range was +22.4±0.5 mV–+37.9±0.3 mV. *In-vitro* drug release investigations revealed a characteristic pH-dependent drug release. The cytotoxicity testing of optimal formulation revealed that the doxorubicin was successfully released from the formulations and exerted therapeutic effect. According to our research, doxorubicin could be loaded onto linear polyamidoamines for potent antitumor effects on the target liver cancer cell lines (Hep G2).

Keywords: Polyamidoamine, doxorubicin, polymeric nanoparticles, liver cancer, cytotoxicity.

INTRODUCTION

In the current era, there have been remarkable improvements in the medicine field due to the perception of nanotechnology, it has decreased potential toxicity as well as the cost of therapy. Nanotechnology has enhanced the specificity, tolerance, efficacy and therapeutic index of many hydrophilic and lipophilic drugs (Sezgin-Bayindir *et al.*, 2021). At the targeted region improved intracellular penetration and drug absorption is achieved due to shielding of nanomedicines from the early disintegration and biological environment which in-return improves the bioavailability and retention time (Sahu *et al.*, 2021). Doxorubicin (DOX), an anthracycline anticancer drug, is frequently used to treat stomach cancer (Sohail *et al.*, 2021), cervical cancer (Robledo-Cadena *et al.*, 2020), hepatocellular carcinoma (Kullenberg *et al.*, 2021), lungs cancer (Kaur *et al.*, 2020) and other human malignancies. Doxorubicin therapeutic action is attributed to DNA damage via two hypothesised mechanisms, including the production of free radicals and the inhibition of topoisomerase II (van der Zanden *et al.*, 2021). However, dose-related myelosuppression and cardiotoxicity limit the usage of DOX in cancer therapy (Lucas *et al.*, 2019). One of the most efficient strategies to decrease their side effects is encapsulating anticancer medications in biodegradable polymers (Yan *et al.*, 2020, Zhao *et al.*, 2018). The PEGylated Liposomal doxorubicin formulation Doxil® was given the approval for marketing by the Food and Drug Administration (FDA), subsequently, post-marketing surveillance demonstrated that the severity of doxorubicin mediated cardiotoxicity and other side effects was reduced, as well as the benefits of targeted drug delivery were achieved. However, at the same time the occurrence of new side effects that were unrelated to doxorubicin, such as stomatitis, and Palmar-Plantar Erythrodysesthesia (PPE) were observed (Zahednezhad *et al.*, 2019). This observation necessitate the development of polymeric nano formulations with some ideal qualities, such as nonimmunogenic, noninflammatory, lack of thrombogenicity and non-toxic.(Ranucci and Manfredi, 2019). Polyamidoamines (PAAs) have various biomedical applications due to the possession of some versatile qualities like biocompatibility, biodegradability, water solubility, low hemolytic toxicity and good peptide-mimicking structures (Ranucci and Manfredi, 2019). Additionally, PAA has the capacity to burst endo/lysosomes and go through structural changes. The cytotoxic potential of PAAs positive charge can be decreased by acetylation/ PEGylation (Ambekar *et al.*, 2020).

DOX was congugated to polyamidoamine dendrimers (PMAM) using an acid-sensitive linker (Guo *et al.*, 2019). While linear polyamidoamines were being researched for gene delivery, dendrimers were used for the majority of the pharmaceuticals. The current work investigated the particle size, zeta potential and DOX release profile of DOX loaded linear PAA based polymeric nanocarriers as well as their cytotoxicity on Hep G2 cells. This study

**Corresponding author:* e-mail: zeeshan.danish.pk@gmail.com

examined how size, zeta potential and drug loading percentage were affected by polymer concentration and PEGylation.

MATERIALS AND METHODS

Materials

For Polymer and co-polymer

Chloroform 99.5% was purchased from BDH, India, Methylene-bis (acrylamide) (MBA) 99% from Sigma Aldrich, Germany, N-N-Dimethylethylenediamine (DMEDA) 97% Arlington, USA, Calcium hydride from Oakwood, chemicals, China, Hydrochloric acid (HCl) 37% from Merck, Germany, Sodium Sulphate >99% from Merck, Germany, Carbonyl di imadazole 98.6% from Chem Impex, USA, 4-methoxy-phenol 98% was purchased from Alfa Aeser, Germany, Monomethoxy Polyethylene Glycol 1900 (PEG) was purchased from Alfa Aeser, USA,

For buffer solutions

Potassium Chloride 99% purity was purchased from BDH, United Kingdom, Potassium phosphate monobasic 95% purity from Merck, Germany, Tris base from Santa Cruz Biotechnology, USA Sodium Chloride >99% from Merck, Germany, Triton X from High Purity Chemicals, Duksan Pure Chemicals, China and Sodium phosphate dibasic 98-105% purity from Merck Germany.

For Nanocarriers

Disodium phosphate 99% purity was purchased from Omicoron, sciences Limited UK, Doxorubicin (DOX) was obtained from Pharmedics Laboratories (PVT) Ltd., Dichloromethane (DCM) 99.8% purity from RdH Labor Chemikalien, Germany, Potassium Chloride 99% purity was purchased from Penta Chemicals, Czech republic, Sodium Chloride 99-100.5% purity from Sigma, Germany, monopotassium phosphate 95% purity from Merck Germany, N,N -dimethylformamide 99.5% purity was purchased from Deajung, China.

For Cytotoxicity

3–(4, 5-dimethylthiazole-2-yl)-2, 5-phenyltetrazolium bromide (MTT) reagent was purchased from Bioshop Canada, Fetal Bovine Serum (FBS) from Capricorn Scientific Germany, Trypsin-EDTA from Sigma Aldrich Germany, Dimethyl Sulfoxide (DMSO) from Duksan Pure Chemicals, Penicillin-Streptomycin (100X) solution was purchased from Caisson Laboratories USA, China and Dulbecco's Modified Eagle's Medium (DMEM) was from Caisson Laboratories USA,

Method

Preparation of NF2

For the preparation of polymer previously described method for NG49 was used with slight modification (Rackstraw *et al.*, 2002). 15 ml distilled water, 5.0 ml DMEDA, 20mg of 4 methoxyphenol and 7.17g MBA were allowed to react at 25°C for two days in a nitrogen environment. After being diluted with distilled water, aqueous HCl was employed to bring the pH to 2. Freeze drying was done after being ultrafiltration through 10,000 DWCO membrane against cold water.

Preparation of NF4

Preparation of Vinyl terminated PAA

A slightly modified version of the previously published NG47 (Rackstraw *et al.*, 2002) was used to prepare the PEGylated Polymer. DMEDA 5ml, 15ml of distilled water and 20mg of 4 methoxyphenol were added in 7.17g MBA and allowed to react for two days at 25°C, in a dark nitrogen atmosphere. Freeze drying was done after being ultrafiltration through 10,000 DWCO membrane against cold water.

Preparation of Amino terminated PEG

30g of monomethoxy-PEG 1900 after being dissolved in 150ml of chloroform was dried over calcium hydride for an entire night, then separated by filtration. 8.31g of carbonyldiimidazole was added while the solution's temperature was maintained at 30°C for 15 minutes and stirred for 10 minutes after the addition of 30ml of ice-cold distilled water. After the phases were separated, to the organic phase DMEDA 7g was added and the reaction was proceeded at 25°C for 24 hours. After being diluted with chloroform (400ml), the organic phase was extracted five times with 80ml of water, dried with sodium sulphate and then concentrated to 100ml in a rotary evaporator. In the resultant solution 500ml of diethyl ether was added. The precipitate that was produced as a result of this operation was filtered and collected before being dried at 0.1 Torr to constant weight.

Preparation of PEG-PAA-PEG Co-polymer

Under nitrogen stream, 2.73g of vinyl-terminated PAA and 1.87g of amino-terminated PEG were added in 5ml of an aqueous solution. The reaction was then proceeded at 25°C for 24 hours. The resulting solution pH was then brought down to 2 by adding 1M HCl after it had been diluted with distilled water. After being ultrafiltered at 5-10°C against a membrane of 50,000 Da, MWCO, it was then freeze-dried.

Yield

Weighing the lyophilized polymers of NF2 and NF4 from three produced batches give the yield in grams (Forte *et al.*, 2021).

Intrinsic viscosity

Oswald's viscometer was used to measure the intrinsic viscosity. Subsequently, several polymer concentration solutions (8%, 4%, 2%, 1%, and 0.5%) were prepared at pH 8.09 in Tris buffer and Equation 1 was used to calculate the relative viscosity (η_r) (Zhang and Feng, 2021).

$$\eta r = \frac{t}{to}$$ Equation 1

Where t is the test solution flow time and t_o is the solvent flow time

Specific viscosity (η_s) could be determined by Equation 2 (Zhang and Feng, 2021)

$$\eta s = \eta r - 1$$ Equation 2

Equation 3 could be used to calculate reduced viscosity (Zhang and Feng, 2021)

$$\eta red = \frac{\eta r}{C}$$ Equation 3

Where "C" denotes the concentration in g/dl

Using the y intercept, the intrinsic viscosity value could then be calculated of the graph between reduced viscosity and concentration.

Fourier transform infrared (FTIR)

Cary 630 FTIR-spectrophotometer by Agilent Technology, was used to conduct the FTIR measurements at range of 4000 to 800 cm^{-1} wave number (Rizzi *et al.*, 2021)

Nuclear magnetic resonance spectroscopy

To capture carbon nuclear magnetic resonance (^{13} C NMR) spectra, the material was dissolved in DMSO solvent and analysed by using a spectrophotometer from 600 MHz Bruker's Advance Neo Technology (Bruker Co., Ltd.).(Smith *et al.*, 2019).

Doxorubicin loaded nanocarriers

Drug was loaded by emulsion solvent evaporation technique as previously described (Nguyen and Hammond, 2006) with slight modifications. After mixing 10 mg of DOX in 1 ml of methanol and 4 ml of DCM with the aid of ultrasound for 10 minutes, the resultant solution was then gradually added (dropwise) to a 10 ml of polymer/co-polymer aqueous solution (10mg/ml, 20 mg/ml, and 30mg/ml). The solution was stirred vigorously all night at room temperature to evaporate the organic phase. The following day, 30 minutes centrifugation at 4500 rpm was performed to remove the precipitated drug. Filtration through a 0.45 µm PTFE syringe filter of the supernatant containing the drug-loaded nano-dispersion was done to remove any remaining precipitated drug. The nano dispersion was lyophilized after that for safe storage. 10 ml of N, N-dimethyl formamide was used to dissolve the nanocarriers, and to measure the absorbance at 480nm using Shimadzu UV-2550 UV-Visible Spectrophotometer (Zhang *et al.*, 2016). The drug concentration was calculated by standard curve method. The Percent Drug loading was determined by the equation 4 (Nguyen and Hammond, 2006) .

$$\text{Percentage drug loading} = \frac{\text{Weight of drug encapsulated}}{\text{Total weight of drug}} \times 100$$ Equation 4

Size and zeta potential

A sample of nanocarriers was analysed using a (Malvern Nano ZSP) Zetasizer after being diluted in a 5mM sodium chloride solution (Janesch *et al.*, 2020)

Scanning electron microscopy

Nova Nano SEM 450 field-emission scanning electron microscope (FE-SEM), was used to observe the surface morphologies of the nanocarriers. SEM analysis of the dried, lyophilized nanocarriers was performed (Batra *et al.*, 2022).

In vitro drug release

In- vitro drug release was studied with slight modifications of previously reported method (Zhang *et al.*, 2016). Doxorubicin-loaded nanocarriers equivalent to 3mg of DOX were dissolved with 5 ml of release medium (pH 7.4 and 5.5, PBS solution) before being put into (10,000 Da MWCO) dialysis bags and tightly closing the ends in order to measure the doxorubicin in-vitro release from the nanocarriers. The release activity was started by inserting the bag into 50ml of release medium with constant stirring. At predefined intervals, a 3ml sample of the release media was removed and replaced with 3ml of fresh media. Standard curve method was used to calculate the amount of DOX released by UV-vis spectro-photometry at 480.

Hemolysis studies

Hemolysis studies was conducted with the slight modification of previously reported method (Lakkadwala and Singh, 2019). Freshly drawn human blood would be centrifuged for 10 minutes at a speed of 1,500 g at a temperature of 4°C. After removing the supernatant, the red blood cells (RBCs) would be rinsed with PBS pH 7.4 and was centrifuged again for 5 min, 4°C and 1500 g. With phosphate buffer saline it was diluted to 4% (v/v). Samples of the RBC samples were stored at 4°C until the experiment and then used within 24 hours. After adding polyamidoamine solution of various known concentrations in PBS (4%, 2%, 1%, 0.5%, and 0.25%) and 1% triton-X, in the RBC sample, it was then incubated for 90 min at 37°C. The absorbance of the supernatant for haemoglobin at 550 nm would then be determined. The Equation 5 was used to calculate haemoglobin release (Lakkadwala and Singh, 2019):

$$\text{Hemoglobin release percent} = \frac{(\text{Abstract} - \text{Abs vehicle}}{\text{Abs Triton} - \text{X} - \text{Abs vehicle}} \times 100$$ Equation 5

Where, Abs Vehicle, Abs Triton-X, and Abs Test denote the absorbance readings of RBCs treated with PBS alone, Triton-X, and from solutions containing various concentrations of polymer respectively.

In-vitro cytotoxicity studies

The human Liver Cancer cell line (Hep-G2) was provided by the CEMB (Lahore), and the cells were cultured in in a 5% CO2, saturated atmosphere in DMEM with 10% FBS

and 1% penicillin-streptomycin at 37°C. After being ultra centrifuged for 5 min at 5000 rpm, when the cells were confluent to an extent of 85-90%, they were subcultured by using trypsin EDTA.

In the beginning, 5×10^3 Hep G2 cells were added to each well of a 96-well microtiter plate. To achieve the proper cell adhesion, the cells were cultured in a CO2 incubator for 24 hours at a temperature of 37°C. Following the addition of polymers (NF2 and NF4) at a concentration of 40 µg/ml to 600 µg/ml and doxorubicin-loaded nano-particle formulation at a concentration of 0.5 to 40 µg/ml (in triplicate), the incubation was then continued for an additional 24 hours. Hep G2 cells grown in DMEM medium (5×10^3 cells/well) were utilised as a control.

The MTT experiment was conducted by adding in each well 1:10 MTT reagent:DMEM medium the reaction was stopped by the addition of 100µl of DMSO in each well of the microtiter plate after 24 hours ,after that, MTT and DMEM medium was removed, and the results were read at 490 nm using an RT-6000 microtiter plate reader (Zhang *et al.*, 2016). The cell viability was calculated using the equation 6 (Lakkadwala and Singh, 2019):

$$\text{Cell viability \%} = \frac{\text{Abs sample}}{\text{Abs control}} \times 100 \qquad \text{Equation 6}$$

STATISTICAL ANALYSIS

The results were presented as Mean ± S.D, calculated on Microsoft Excel 2016.

Ethical approval

The study was approved by Punjab University Institutional Ethics Review Board vide No.D/006/FIMS.

RESULTS

Yield and Intrinsic viscosity of Polymers

The average yield of the polymers NF2 and NF4 was 11.5 ±0.95g and 4.4 ±0.5g respectively, the calculated intrinsic viscosity value for NF2 and NF4 was 0.793 and 0.315 dl/g respectively, whereas, in the literature, the 0.15 to 1 dl/g intrinsic viscosity range was reported (Ferruti, 2013).

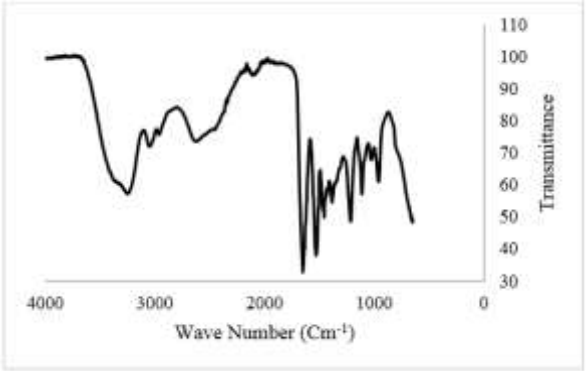

Fig. 1: FTIR of NF2

FTIR

In the FTIR of NF2 (fig. 1), the amide group C-H stretching and N-H bending (1533 cm^{-1}), amide group C=O stretching (1653 cm^{-1}) and amine group N-H stretching (3257 cm^{-1}). This was comparable to previously reported polyamidoamine FTIR, which supported the CONHR group from N-H bending at 1530-1560 cm^{-1} and N-H stretching at 3250-3300cm^{-1} and C=O stretching at 1640-1680 (Vatanpour and Sanadgol, 2020).

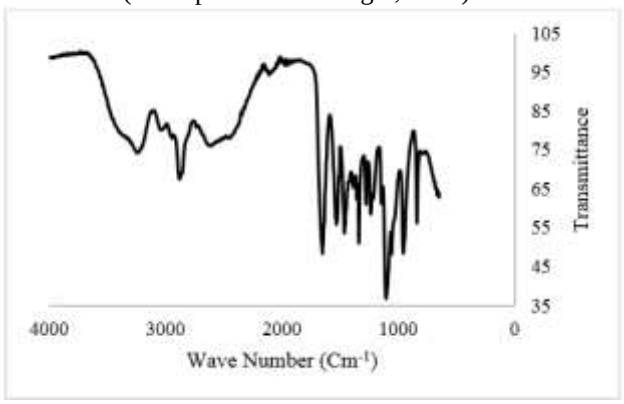

Fig. 2: FTIR of NF4

In the FTIR of NF4, Fig. 2, amide group C-N-H of in-plane vibrations (1533 cm^{-1}), amide group C=O stretching (1653cm^{-1}), amine group N-H stretching (3254cm^{-1}). C-O-C group stretching vibrations (1107 cm^{-1}), C-H group bending (1339 and 1464 cm^{-1}) and C-H group asymmetric stretching (2883 cm^{-1}). This was comparable to the FTIR of PEG, C-H stretching (2886 cm^{-1}) and stretching of C-O group of PEG (1104 cm^{-1}) (Ho *et al.*, 2019).

^{13}C NMR

Chemical shifts of ^{13}C NMR of NF4 is as follow, in DMSO δ_C 29.43, δ_C 39.08, δ_C 39.21, δ_C 39.35, δ_C 39.49, δ_C 39.63, δ_C 39.77, δ_C 39.91, δ_C 43.66, δ_C 48.79, δ_C 51.49, δ_C 58.06, δ_C 60.19, δ_C 69.59, δ_C 69.78, δ_C 71.23, δ_C 72.33, δ_C 119.17, δ_C 169.13

Chemical shift at δ 69.59 ppm corresponds to the PEG, which indicate the successfully attachment PEG to PAA polymer. This observation was similar with the previously reported chemical shifts of ^{13}C NMR of DMEDA-PEG-DMEDA-(MBA-DMEDA) $_{n+1}$-PEG-DMEDA (Parkhouse *et al.*, 2008)

Drug Loading

Standard curve method was used for the calculation of percentage of drug loading at 480nm. The percentage drug loading by all formulations in DOX-to-polymer/co-polymer ratios (1:10, 1:20 and, 1:30) was ≥ 90% as shown in the Table 1.

Size and Zeta Potential

The nanoparticle diameter following DOX loading was ranged 245 ± 1.10 nm–579 ± 1.00 nm as shown in Table 2. The diameter of nanoparticles was decreased with the

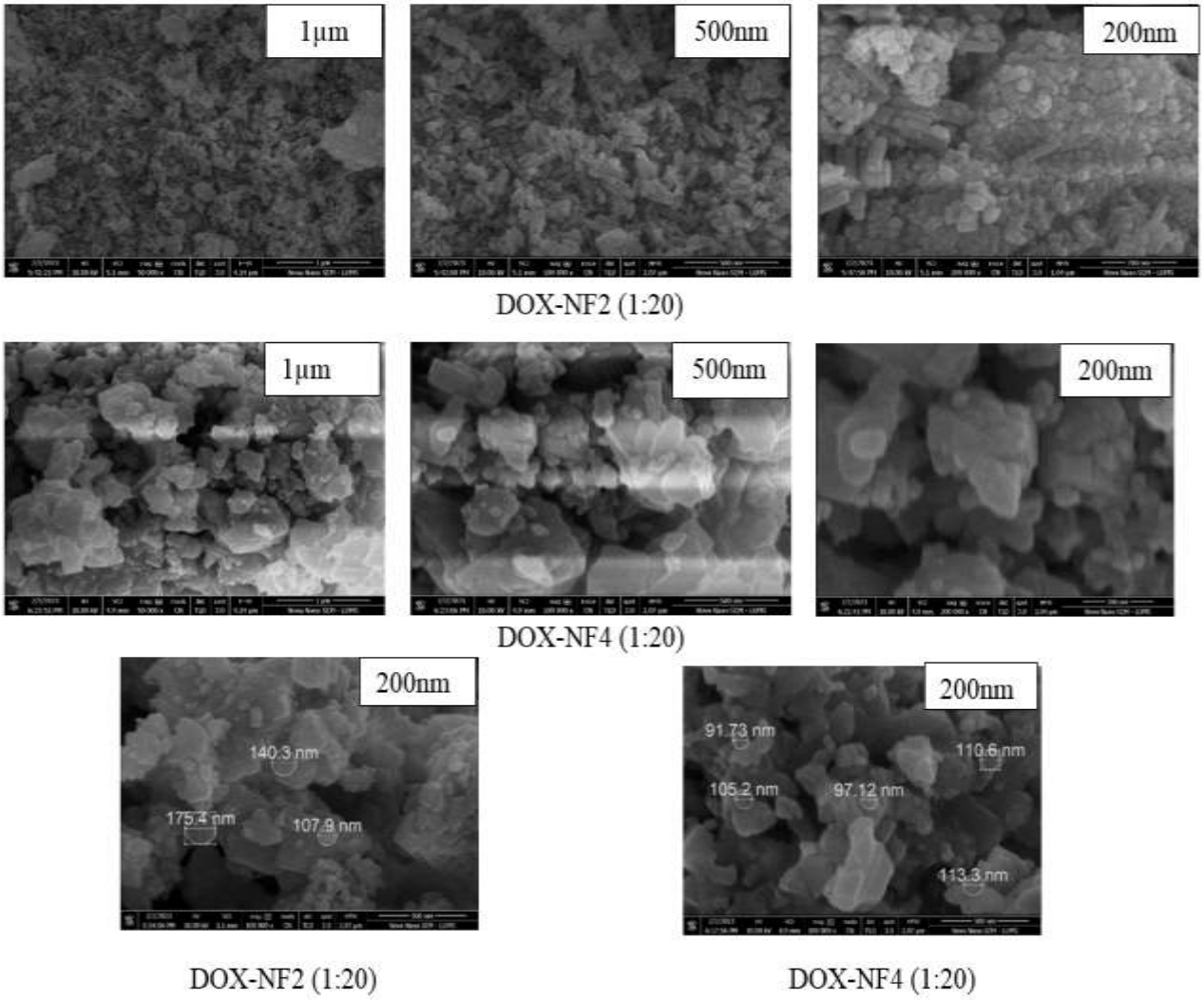

Fig. 3: SEM image of DOX-NF2 (1:20) and DOX-NF4 (1:20)

Table 1: Percentage Dug loading by NF2 and NF4

Polymer	Doxorubicin (mg)	Polymer (mg)	Drug: Polymer	Percentage Drug Loading
NF2	10	100	1:10	95.17 ± 0.99
NF2	10	200	1:20	95.40 ± 1.85
NF2	10	300	1:30	93.67 ± 1.15
NF4	10	100	1:10	93.20± 1.18
NF4	10	200	1:20	94.50± 0.62
NF4	10	300	1:30	95.53± 1.79

Table 2: Diameter, PDI and Zeta Potential of different formulations DOX-NF2 and DOX-NF4

Sr. No	Formulation	Size Diameter (nm)	Polydispersity Index (PDI)	Potential (mv)
1	DOX-NF2 (1:10)	324 ± 1.01	0.636 ± 0.052	+33.5 ± 0.4
2	DOX-NF2 (1:20)	278 ± 0.95	0.349 ± 0.044	+25.4 ± 0.9
3	DOX-NF2 (1:30)	308 ± 1.04	0.501 ± 0.027	+37.9 ± 0.3
4	DOX-NF4 (1:10)	387 ± 0.95	0.403 ± 0.150	+22.4 ± 0.5
5	DOX-NF4 (1:20)	245 ± 1.10	0.454 ± 0.029	+29.6 ± 1.2
6	DOX-NF4 (1:30)	579 ± 1.00	0.613 ± 0.019	+32.0 ± 1.6

increase in DOX to polymer/co-polymer ratio from 1:10 to 1:20 this was similar with the previously described outcomes which showed that the polyplexes diameter was decreased with increase in polymer concentration (Rackstraw *et al.*, 2002).

It was observed, with the further increase in DOX to polymer/co-polymer ratio, i.e., 1:30 that the diameter of nanocarriers was increased instead of further decreasing. A positive zeta potential value was observed for all formulations, from +22.4±0.5 mV–+37.9±0.3 mV, shown in Table 2, indicating good stability, the stability was enhanced due to repulsion of oppositely charged particles (Li *et al.*, 2021). The zeta potential of non-PEGylated formulation of DOX-NF2 (1:10 & 1:30) was observed +33.5±0.4 & +37.9±0.3 greater than the PEGylated formulation DOX-NF4 in the same DOX to co-polymer ratio +22.4 ± 0.5 & +32.0±1.6. Whereas, the zeta potential of DOX-NF2 (1:20) was +29.7 ± 0.9 almost equal to the DOX-NF4 (1:20) i.e. +29.6±1.2.

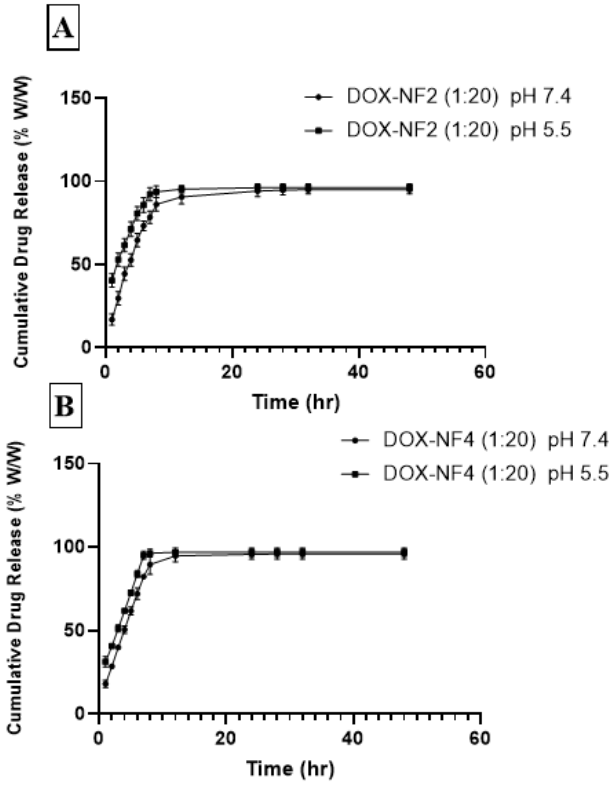

Fig 4: Percentage (W/V), Cumulative Drug Release at pH 7.4 and 5.5 (A) DOX-NF2 (1:20), (B) DOX-NF4 (1:20) drug to polymer ratios respectively.

The morphology of nanocarriers was exhibited in the SEM images of DOX-NF2 (1:20) and DOX-NF4 (1:20), as shown in fig. 3 nanocarriers DOX-NF2 (1:20) was roughly spherical. The morphology of the nanocarriers DOX-N4 (1:20) was random, and the variance in the sizes of the nanocarriers was also clearly discernible

In-vitro drug release

In order to treat cancer successfully, the drug must reach the tumour cells with the possibility of minimum drug release during circulation. The DOX release was somewhat increased in the acidic endosome environment compared to physiological pH. After 3 hours, the total DOX release from the optimum formulations DOX-NF2 (1:20) and DOX-NF4 (1:20) was lower 44.40±4.0 % & 40.00±1.0 % in pH 7.4 PBS, than the pH, 5.5 61.69± 4.0% & 51.35±2.1% as shown in Fig 4. The percentage drug release after 6 hours at pH 7.4 of DOX-NF2 (1:20) and DOX-NF4-(1:20) was 73.32±2.9 and 72.08±3.4 and at pH 5.5 was 85.81±4.5 and 83.97±2.1 respectively. After the 6 hours the percentage drug release at both pH (7.4 & 5.5) was almost comparable.

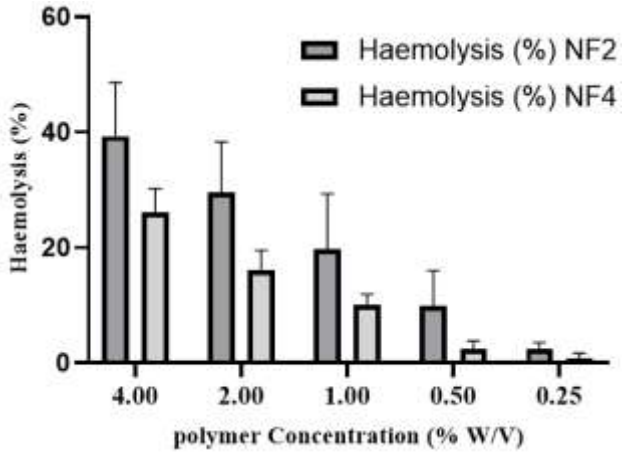

Fig. 5: Haemolysis (%W/V) of polymer NF2 and NF4 at 0.25%, 0.5%, 1%, 2% and 4%, respective polymer concentration

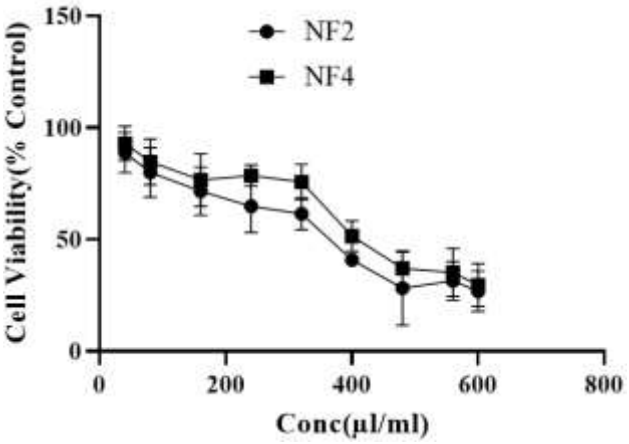

Fig. 6: Cytotoxicity studies conducted against Hep-G2 cell lines of NF2 and NF4

Haemolysis

The percent haemolysis of NF2 and NF4 was 39.34±9.3, and 26.09±4.1 respectively at the 4% polymeric concentration. Whereas, at 2% concentration it was reduced to 29.53±8.8 and 16.01±3.5 As shown in Fig. 5.

In-vitro Cytotoxicity

As shown in Fig. 6, IC_{50} for NF2 and NF4 was 203.8µg/ml and 268.3µg/ml, the maximum haemolytic toxicity and cytotoxicity was observed for polymer NF2, after PEGylation of NF2, the haemolytic toxicity and cytotoxicity of resultant NF4 was reduced.

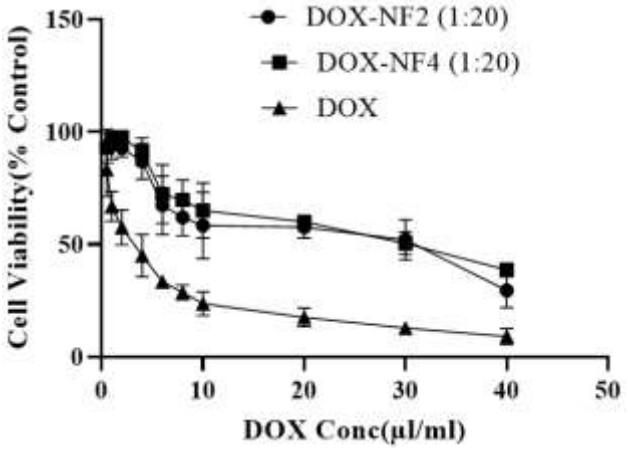

Fig. 7: Cytotoxicity studies of DOX-NF2 (1:20) and DOX-NF4 (1:20) and DOX on Hep-G2 cell line

The IC 50 values for free DOX, DOX-NF2 and DOX-NF4 (1:20) were 11.08µg/ml, 9.93µg/ml and 3.28µg/ml respectively as shown in Fig. 7, These outcomes showed that doxorubicin was successfully liberated from the formulation and produce its therapeutic effect.

DISCUSSION

Some of the potential methods for encapsulation or drug loading in the polymer include electrostatic interactions, physical encapsulation, hydrophobic interactions and hydrogen bonds (Zielinska *et al.*, 2020). However, drugs could be potentially conjugated by a covalent bond or electrostatically attached externally (Guo *et al.*, 2019). Doxorubicin has extremely low amphipathic properties (pKa 8.3), making it extremely difficult to encapsulate. Anionic polymers were used to load the DOX in some studies (Yi *et al.*, 2018). The efficiency of co-encapsulating DOX with ammonium sulphate or using negatively charged polymers both demonstrated a considerable improvement in DOX encapsulation. Doxorubicin was incorporated as magnetic polymeric nanoparticles by adopting the double emulsion solvent evaporation technique, which is used to encapsulate both hydrophobic and hydrophilic medications (Khizar *et al.*, 2020).

It is clear from the literature that the ability for the amide group or tertiary amine group to form hydrogen bonds with drug molecules containing particular atoms, such as oxygen or nitrogen or groups, such as hydroxyl group or carboxy (Abedi-Gaballu *et al.*, 2018). Hydrophobic doxorubicin base (DOX) was loaded in this study using the emulsification solvent evaporation method. The hydrogen bonding between the oxygen atom of the doxorubicin and the (N-H) of the amide group and physical encapsulation of the drug by the polymer are two potential drug loading mechanisms.

The size of the nanoparticles is crucial because they must get through the vascular endothelial tight junction in order to enter the cells. The bioavailability and intracellular penetration of nanoparticles are largely influenced by their surface charge and particle size (Zhao and Stenzel, 2018). ERP (increased permeability and retention effect) is visible in some cancer types where the endothelium becomes leaky and even loses the lymphatics, allowing material to pass through the endothelial and enter the tissue (Dadwal *et al.*, 2018). Nanoparticles are frequently removed by the mononuclear phagocytic system. In order to prevent the removal of nanoparticles by the mononuclear phagocytic system, they must be coated with hydrophilic surface groups that repel plasma proteins (Reichel *et al.*, 2019).

Although, as demonstrated in Table 2 polymer concentration has a direct impact on zeta size. The lack of a discernible trend in particle diameter for the presence or absence of PEG is the consequence of the preparation procedure. This discovery matched observations made in the literature that the nanoparticles produced by the nanoprecipitation or emulsion methods either in the absence of surfactants or at lower concentrations were discovered to produce a range of nanoparticle sizes (Crucho and Barros, 2017).

As depicted in Table 2, the increase in polymer concentration does not directly correspond to an increase in the zeta potential. According to previous studies, the zeta potential is influenced by pH, the nature of buffer, and salt concentration, all of which could mitigate the effects of the PEG layer. (Teulon *et al.*, 2018). Previous research demonstrated that comparing results from different contexts is still difficult. For instance, it has been demonstrated that PEGylation of PLA or PLGA nanoparticles minimally alters their zeta potential, which nevertheless remains strongly negative despite the addition of generous amounts of PEG (Zamanlu *et al.*, 2019).

The result of zeta potential as shown in Table 2 indicate that PEG has successfully shielded the surface charge of the particles, this observation was same for the previously reported study of paclitaxel loaded polyamidoamine based dendrimers (Bhatt *et al.*, 2019).

Initially for 6 hours the cumulative percentage drug release at pH 7.4 was slower than the cumulative percentage drug release at pH 5.5 for DOX-NF2 (1:20) and DOX-NF4 (1:20), then, the drug release at both pH

become almost comparable. In an acidic environment, DOX became more water soluble, which was one potential cause. The outstanding anti-tumor therapeutic potential of the DOX-loaded nano-formulations was demonstrated by pH-responsive DOX release behaviour. As opposed to physiological pH, the release of drugs would be greatly accelerated at acidic pH, endosomal/lysosomal pH (Dong *et al.*, 2018).

Interaction of positively charged structures and erythrocyte membrane which leads to the rupture of the erythrocytic membrane is the proposed mechanism for hemolysis. Serum addition significantly reduces the hemolytic ability of the previously described PAA, polymer of (MBA-DMEDA), showing that the polymer's structure has a significant impact on the interactions between serum and polycations. The results demonstrated that PEGylation significantly reduce the % hemolysis. Therefore, it is essential to hide the polyamidoamine charge in order to get the desired outcomes. Value for percent haemolysis of NF4 after NF2's PEGylation was dramatically reduced, as previously reported that acetylation or PEGylation could reduce cytotoxicity (Nair *et al.*, 2023). Because macromolecules frequently enter cells through the process of endocytosis, this could be the cause of the cytotoxicity. Endocytosis exposes macromolecules to pH changes from (pH 7.4) extracellular to (pH 5.5-6.5) endosomal lysosomal system. This pH variation would cause conformational changes and possible exposure (Xu *et al.*, 2021).

Similar to our results, earlier investigations, those done on Hep G2 cell lines revealed that the IC_{50} values of liposomal DOX were higher than those of free DOX because the drug was released more slowly following the degradation of the liposomes (Kullenberg *et al.*, 2021).

CONCLUSION

In this study the drug loading efficiency of DOX by the linear polyamidoamine and its PEGylated co-polymer were studied by varying the concentration of polymer and co-polymer. The results showed that all the polymers/co-polymers loaded the drug with excellent drug loading efficiencies. Studies on drug release *in vitro* revealed that the drug's release is somewhat enhanced with an acidic pH, demonstrating the formulation sensitivity to pH. According to in-vitro cytotoxicity results, the doxorubicin was successfully released and had a therapeutic impact on Hep G2 cells, indicating that it could be used to treat Hep G2 cell carcinomas.

ACKNOWLEDGEMENTS

Centre for Excellence in Molecular Biology (CEMB), Lahore is acknowledged for providing the established liver cancer cell lines (Hep G2) and Pharmedics Laboratories (Pvt.) Ltd. is acknowledged for providing the doxorubicin free base (DOX).

REFERENCES

Abedi-Gaballu F, Dehghan G, Ghaffari M, Yekta R, Abbaspour-Ravasjani S, Baradaran B, Dolatabadi JEN and Hamblin MR (2018). PAMAM dendrimers as efficient drug and gene delivery nanosystems for cancer therapy. *Appl. Mater. Today*, **12**(3): 177-190.

Ambekar RS, Choudhary M and Kandasubramanian B (2020). Recent advances in dendrimer-based nanoplatform for cancer treatment: A review. *Eur. Polym. J.*, **126**(5): 109546.

Batra NM, Mahalingam DK, Doggali P, Nunes SP and Costa PM (2022). Investigating the thermal stability of metallic and non-metallic nanoparticles using a novel graphene oxide-based transmission electron microscopy heating-membrane. *Nanotechnology*, **33**(25): 255701.

Bhatt H, Kiran Rompicharla SV, Ghosh B and Biswas S (2019). α-tocopherol succinate-anchored PEGylated Poly (amidoamine) dendrimer for the delivery of paclitaxel: assessment of *in vitro* and *in vivo* therapeutic efficacy. *Mol. Pharm.*, **16**(4): 1541-1554.

Crucho CI and Barros MT (2017). Polymeric nanoparticles: A study on the preparation variables and characterization methods. *Mater. Sci. Eng. C*, **80**(11): 771-784.

Dadwal A, Baldi A and Kumar Narang R (2018). Nanoparticles as carriers for drug delivery in cancer. *Artif. Cells Nanomed. Biotechnol.*, **46**(2): 295-305.

Dong J, Wang K, Sun L, Sun B, Yang M, Chen H, Wang Y, Sun J and Dong L (2018). Application of graphene quantum dots for simultaneous fluorescence imaging and tumor-targeted drug delivery. *Sens. Actuators B Chem.*, **256**(3): 616-623.

Ferruti P (2013). Poly (amidoamine) s: Past, present, and perspectives. *J. Polym. Sci. A Polym. Chem.*, **51**(11): 2319-2353.

Forte C, Alongi J, Beduini A, Borsacchi S, Calucci L, Carosio F, Ferruti P and Ranucci E (2021). The thermo-oxidative behavior of cotton coated with an intumescent flame retardant glycine-derived poly-amidoamine: A multi-technique study. *Polymers*, **13**(24): 4382.

Guo XL, Kang XX, Wang YQ, Zhang XJ, Li CJ, Liu Y and Du LB (2019). Co-delivery of cisplatin and doxorubicin by covalently conjugating with polyamidoamine dendrimer for enhanced synergistic cancer therapy. *Acta Biomater.*, **84**(1): 367-377.

Ho MN, Bach LG, Nguyen TH, Ho MH, Nguyen DH, Nguyen CK, Nguyen CH, Nguyen NV and Hoang Thi TT (2019). PEGylated poly (amidoamine) dendrimers-based drug loading vehicles for delivering carboplatin in treatment of various cancerous cells. *J. Nanopart. Res.*, **21**(2): 1-12.

Janesch J, Czabany I, Hansmann C, Mautner A, Rosenau T and Gindl-Altmutter W (2020). Transparent layer-by-layer coatings based on biopolymers and CeO2 to protect wood from UV light. *Prog. Org. Coat.*, **138**(1): 105409.

Kaur P, Mishra V, Shunmugaperumal T, Goyal AK, Ghosh G and Rath G (2020). Inhalable spray dried lipidnanoparticles for the co-delivery of paclitaxel and doxorubicin in lung cancer. *J. Drug Deliv. Sci. Technol.*, **56**(2): 101502.

Khizar S, Ahmad NM, Ahmed N, Manzoor S and Elaissari A (2020). Encapsulation of doxorubicin in magnetic‐polymer hybrid colloidal particles of Eudragit E100 and their hyperthermia and drug release studies. *Polym. Adv. Technol.*, **31**(8): 1732-1743.

Kullenberg F, Degerstedt O, Calitz C, Pavlovic N, Balgoma D, Gråsjö J, Sjögren E, Hedeland M, Heindryckx F and Lennernäs H (2021). In vitro cell toxicity and intracellular uptake of doxorubicin exposed as a solution or liposomes: Implications for treatment of hepatocellular carcinoma. *Cells*, **10**(7): 1717.

Lakkadwala S and Singh J (2019). Co-delivery of doxorubicin and erlotinib through liposomal nanoparticles for glioblastoma tumor regression using an in vitro brain tumor model. *Colloids Surf. B-Biointerfaces*, **173**(1): 27-35.

Li Z, Lin Q, Mcclements DJ, Fu Y, Xie H, Li T and Chen G (2021). Curcumin-loaded core-shell biopolymer nanoparticles produced by the pH-driven method: Physicochemical and release properties. *Food Chem.*, **355**(22): 129686.

Lucas A, Lam D and Cabrales P (2019). Doxorubicin-loaded red blood cells reduced cardiac toxicity and preserved anticancer activity. *Drug Deliv.*, **26**(1): 433-442.

Nair A, Javius-Jones K, Bugno J, Poellmann MJ, Mamidi N, Kim I-S, Kwon IC, Hong H and Hong S (2023). Hybrid nanoparticle system integrating tumor-derived exosomes and poly (amidoamine) dendrimers: implications for an effective gene delivery platform. *Chem. Mater.*, **35**(8): 3138-3150.

Nguyen PM and Hammond PT (2006). Amphiphilic linear-dendritic triblock copolymers composed of poly (amidoamine) and poly (propylene oxide) and their micellar-phase and encapsulation properties. *Langmuir*, **22**(18): 7825-7832.

Parkhouse SM, Garnett MC and Chan WC (2008). Targeting of polyamidoamine–DNA nanoparticles using the Staudinger ligation: Attachment of an RGD motif either before or after complexation. *Bioorg. Med. Chem.*, **16**(13): 6641-6650.

Rackstraw BJ, Stolnik S, Davis SS, Bignotti F and Garnett MC (2002). Development of multicomponent DNA delivery systems based upon poly (amidoamine)-PEG co-polymers. *BBA-Gene Struct. Expr.*, **1576**(3): 269-286.

Ranucci E and Manfredi A (2019). Polyamidoamines: Versatile bioactive polymers with potential for bio-technological applications. *Chem. Afr.*, **2**(2): 167-193.

Reichel D, Tripathi M and Perez JM (2019). Biological effects of nanoparticles on macrophage polarization in the tumor microenvironment. *Nanotheranostics*, **3**(1): 66.

Rizzi V, Gubitosa J, Fini P, Fraix A, Sortino S, Agostiano A and Cosma P (2021). Development of Spirulina sea-weed raw extract/polyamidoamine hydrogel system as novel platform in photodynamic therapy: Photostability and photoactivity of chlorophyll a. *Mater. Sci. Eng. C*, **119**(2): 111593.

Robledo-Cadena DX, Gallardo-Perez JC, Davila-Borja V, Pacheco-Velazquez SC, Belmont-Diaz JA, Ralph SJ, Blanco-Carpintero BA, Moreno-Sanchez R and Rodriguez-Enriquez S (2020). Non-steroidal anti-inflammatory drugs increase cisplatin, paclitaxel, and doxorubicin efficacy against human cervix cancer cells. *Pharmaceuticals*, **13**(12): 463.

Sahu T, Ratre YK, Chauhan S, Bhaskar L, Nair MP, Verma HK and Technology (2021). Nanotechnology based drug delivery system: Current strategies and emerging therapeutic potential for medical science. *J. Drug Deliv. Sci. Technol.*, **63**(3): 102487.

Sezgin-Bayindir Z, Losada-Barreiro S, Bravo-Díaz C, Sova M, Kristl J and Saso L (2021). Nanotechnology-based drug delivery to improve the therapeutic benefits of NRF2 modulators in cancer therapy. *Antioxidants*, **10**(5): 685.

Smith RJ, Gorman CB and Menegatti S (2019). DendriPeps: Expanding dendrimer functionality by hybridizing poly (amidoamine)(PAMAM) scaffolds with peptide segments. *Macromol. Rapid Commun.*, **40**(22): 1900325.

Sohail M, Sun Z, Li Y, Gu X and Xu H (2021). Research progress in strategies to improve the efficacy and safety of doxorubicin for cancer chemotherapy. *Expert Rev. Anticancer Ther.*, **21**(12): 1385-1398.

Teulon J-M, Godon C, Chantalat L, Moriscot C, Cambedouzou J, Odorico M, Ravaux J, Podor R, Gerdil A and Habert A (2018). On the operational aspects of measuring nanoparticle sizes. *Nanomaterials*, **9**(1): 18.

Van Der Zanden SY, Qiao X and Neefjes J (2021). New insights into the activities and toxicities of the old anticancer drug doxorubicin. *FEBS J.*, **288**(21): 6095-6111.

Vatanpour V and Sanadgol A (2020). Surface modification of reverse osmosis membranes by grafting of polyamidoamine dendrimer containing graphene oxide nanosheets for desalination improvement. *Desalination*, **491**(19): 114442.

Xu W, Luo FQ, Tong QS, Li JX, Miao WM, Zhang Y, Xu CF, Du JZ and Wang J (2021). An intracellular pH-actuated polymer for robust cytosolic protein delivery. *CCS Chem.*, **3**(12): 431-442.

Yan L, Shen J, Wang J, Yang X, Dong S and Lu S (2020). Nanoparticle-based drug delivery system: A patient-friendly chemotherapy for oncology. *Dose Response*, **18**(3): 1559325820936161.

Yi M, Lu Q, Zhao Y, Cheng C and Zhang S (2018). Synthesis and self-assembly of the pH-responsive anionic copolymers for enhanced doxorubicin-loading capacity. *Langmuir*, **34**(26): 7877-7886.

Zahednezhad F, Saadat M, Valizadeh H, Zakeri-Milani P and Baradaran B (2019). Liposome and immune system interplay: Challenges and potentials. *J. Control. Release*, **305**(13): 194-209.

Zamanlu M, Eskandani M, Barar J, Jaymand M, Pakchin PS and Farhoudi M (2019). Enhanced thrombolysis using tissue plasminogen activator (tPA)-loaded PEGylated PLGA nanoparticles for ischemic stroke. *J. Drug Deliv. Sci. Technol.*, **53**(5): 101165.

Zhang H and Feng Y (2021). Dependence of intrinsic viscosity and molecular size on molecular weight of partially hydrolyzed polyacrylamide. *J. Appl. Polym. Sci.*, **138**(34): 50850.

Zhang Y, Xiao C, Ding J, Li M, Chen X, Tang Z, Zhuang X and Chen X (2016). A comparative study of linear, Y-shaped and linear-dendritic methoxy poly (ethylene glycol)-block-polyamidoamine-block-poly (L-glutamic acid) block copolymers for doxorubicin delivery *in vitro* and *in vivo*. *Acta Biomater.*, **40**(12): 243-253.

Zhao CY, Cheng R, Yang Z and Tian ZM (2018). Nanotechnology for cancer therapy based on chemotherapy. *Molecules*, **23**(4): 826.

Zhao J and Stenzel MH (2018). Entry of nanoparticles into cells: The importance of nanoparticle properties. *Polym. Chem.*, **9**(3): 259-272.

Zielinska A, Ferreira NR, Feliczak-Guzik A, Nowak I and Souto EB (2020). Loading, release profile and accelerated stability assessment of monoterpenes-loaded solid lipid nanoparticles (SLN). *Pharm. Dev. Technol.*, **25**(7): 832-844.